

Theoretical study of H chemisorption on NiO. Perfect surfaces and cation vacancies

G. Timothy Surratt and A. Barry Kunz

Department of Physics and Materials Research Laboratory, University of Illinois at Urbana-Champaign, Urbana, Illinois 61801

(Received 28 July 1978)

Self-consistent Hartree-Fock and generalized-valence-bond calculations have been performed using a cluster model for H chemisorption on a NiO (001) surface. The binding energy of the H to Ni or O sites on the surface is found to be less than 0.75 eV while the binding energy to a cation vacancy on the (001) surface and on a crystallite corner is found to be 5.3–7.7 eV. These strongly bonded structures are found to be surface OH⁻ radicals.

I. INTRODUCTION

Experimental studies of chemisorption of CO and O₂ on highly divided NiO catalysts, as well as the catalytic decomposition of N₂O and oxidation of CO by Gravelle and Teichner,¹ indicate that the NiO surface has a number of interesting properties. In the case of O₂ chemisorption, a very large initial heat of adsorption is found (60–114 kcal/mol), but the maximum surface coverage is small, typically a few percent. Successive treatments of NiO with CO indicate that different sites for CO chemisorption exist, since the first chemisorption yields different heats than the second, third, etc. Furthermore, overall activity increases greatly in going from 200 to 250 °C, which has been attributed to increased ionic mobility. Perhaps even more intriguing is the study by Charman and Dell² of chemisorption of H₂, O₂, and N₂O on neutron-irradiated NiO and MgO. They find that the two materials behave in similar fashion despite the obvious differences in the electronic structure of the cation. Their work also illustrates the role of defects in chemisorption on these materials.

In this work we are interested in studying the electronic structure of various configurations of the NiO surface and how this structure effects the chemisorptive properties of the surface. In particular, we are interested in anion and cation sites on the surface and in various vacancy sites on the surface. Of special interest is the role of the transition-metal ion in this system. This paper deals with the perfect surface and cation vacancy sites, while a later paper will deal with anion vacancy sites. A preliminary report of some of this study was published elsewhere.³

The electronic structure of NiO is probably best understood in terms of the properties of its constituent Ni²⁺ and O²⁻ ions. In other work we found that a cluster model NiO (Ref. 4) and CoO (Ref. 5) produces an electronic structure in better agreement with experiment than traditional band-theory

models. In particular, the solid is composed of Ni²⁺ and O²⁻ ions. The O-2*p* states form a valence band but the Ni 3*d* states are essentially noninteracting and atomic (ionic) in character. The electronic structure of the surface then depends on how the surface or surface defects modify the bulk structure.

For the case of the perfect (001) surface, very little change is expected. The Madelung potential is slightly weaker but the overall structure should be the same. If one has a vacancy on the (001) surface, things are considerably different. The effect is toward the formation of O⁻ or Ni⁺ ions immediately surrounding the vacancy. This, in turn, would effect chemisorption on the surface as follows: On the perfect surface one has O²⁻ and Ni²⁺ ions. The O²⁻ is isoelectronic with Ne and thus will not form a strong chemical bond. O⁻, however, is isoelectronic with F and thus strong bonds are expected. The case of the nickel ions is a bit less straightforward. Until recently the *d* electrons of the transition metals were thought to play the dominant role in chemisorption. Recent theoretical⁶ and experimental⁷ studies have indicated that this may not be the case for the first transition series (Sc–Zn). In fact, these studies indicate that the *s*-like electrons of the transition metal are responsible for the chemisorptive bond for this series. Assuming this to be the case for the Ni ions as well, we note that Ni²⁺ has a (3*d*)⁸ configuration, and thus by the *s*-electron ansatz should produce no strong bonds. The Ni⁺ ion has a (3*d*)⁹ ground state, which should also be inert, but also has a (3*d*)⁸(4*s*) excited state, which is ~1 eV above the ground state. It may be possible to bond to this low-lying excited state. The result of this analysis is that we predict that the perfect surface is fairly inert, while the surface defects are active.

This study employs a cluster model for the NiO surface and a single H atom as the adsorbate. The

calculations reported here were all done using *ab initio* self-consistent techniques. As mentioned above, a similar cluster model for NiO and CoO has been quite successful.

In Sec. II we will discuss the computational details. In Sec. III the results are presented and they are discussed in Sec. IV. Finally we present our conclusions in Sec. V.

II. COMPUTATIONAL DETAILS

NiO is an ionic solid composed of Ni²⁺ and O²⁻ ions in the rocksalt structure with a Ni-O distance of 2.09 Å (3.93 a.u.).⁸ In this study we employ small clusters of Ni and O ions embedded in a point-ion field as a model for the solid surface. The point-ion array is a 5×5×4 matrix (charge ±2) that provides (i) charge neutrality and (ii) the correct Madelung potential for the clusters. At the center of the 5×5 (001) face, the Madelung potential is accurate to 0.5% and the average deviation within the surface Ni vacancy cluster is ~1.2%.

Within the framework of performing self-consistent calculations, three different wave functions were employed: restricted Hartree-Fock (RHF), unrestricted Hartree-Fock (UHF), and generalized valence bond (GVB). By RHF we mean the wave function of the form

$$A(\phi_1\alpha\phi_1\beta\phi_2\alpha\phi_2\beta\cdots\phi_m\alpha\phi_m\beta\phi_{m+1}\alpha\cdots\phi_n\alpha), \quad (1)$$

where A is the antisymmetrizer and the ϕ_i may be required to be symmetry functions. The ϕ_i are required to be mutually orthogonal. The UHF wave function is of the form

$$A(\phi_1\alpha\phi_2\alpha\cdots\phi_n\alpha\phi_{n+1}\beta\cdots\phi_{n+m}\beta), \quad (2)$$

where the ϕ_i are not required to be symmetry functions and the up-spin and down-spin orbitals are separately mutually orthogonal. The GVB wave function used here is the perfect pairing form of the GVB wave function⁹ and is an explicitly pairwise correlated wave function. This GVB wave function is obtained from (i) by replacing one or more doubly occupied orbital pair $\phi_i\alpha\phi_i\beta$ with the singlet-coupled pair function $(\phi_{ia}\phi_{ib} + \phi_{ib}\phi_{ia})(\alpha\beta - \beta\alpha)$, where $\langle\phi_{ia}|\phi_{ib}\rangle \neq 0$, but the orbitals of different pairs are taken to be orthogonal. The ϕ_i are solved for variationally and self consistently in each case. The ϕ_i are expanded in terms of a basis of contracted Cartesian Gaussian functions. The basis for Ni is a 4s3p1d basis of Basch, Hornback, and Moskowitz,¹⁰ while the O basis is due to Kunz and Guse¹¹ and is given in Table I. The same programs were used for the calculations as in Ref. 3.

The clusters used for the surface calculations are shown in Fig. 1. The motivation for the sur-

face O and Ni clusters is as follows: the O²⁻ ion is fairly large, while the Ni²⁺ is small. As the H approaches atop an O²⁻ on the surface, it will interact primarily with the O²⁻ and will not be affected by the details of the surface Ni²⁺ charge densities. Thus only the backing Ni²⁺ is included in the surface to allow the d_z^2 to interact through the O²⁻. As an H approaches atop a Ni²⁺ on the surface, however, it will interact with the neighboring surface O²⁻ ions, due to their larger size, as well as with the Ni²⁺ ion. Thus in this case five surface atoms are used as the clusters. The Ni vacancy is modeled by the surrounding five O²⁻ ions. As noted in Fig. 1, three sites above the vacancy were considered. These were atop a surface O, bridged between two surface O's and in the center of the vacancy that is atop a second layer O.

In addition, a set of calculations was done for a Ni vacancy on a crystallite corner. Again the 5×5×4 field was used; however, now the cluster consists of the three O²⁻ ions on a (111) face just below the missing corner Ni²⁺.

III. RESULTS

The potential-energy curves for H approaching atop a surface O (NiOH) and a surface Ni (O₄NiH) are given in Table II and Fig. 2. For the O₄NiH case, both UHF and RHF and GVB curves were calculated. The UHF curves (middle) give the $S_z = \frac{1}{2}$ state slightly below the $S_z = \frac{3}{2}$; however, both are basically repulsive curves. The RHF curve (bottom) for the quartet is essentially the same as the UHF curve for $S_z = \frac{3}{2}$, while the GVB curve, in which the Ni 3d_{z²} and the H 1s are singlet coupled, is somewhat different. For the NiOH case (top), only RHF and GVB curves were calculated. Here we find that the two curves are parallel, with the

TABLE I. Coefficients and exponents for the contracted Cartesian Gaussian basis functions for O²⁻.

Basis function	Exponent	Coefficient
1s	1928.5	0.006 67
	290.39	0.049 36
	66.134	0.211 41
	18.653	0.488 62
	5.9768	0.375 04
2s	1.5	0.821 26
	0.5618	0.097 76
3s	0.1	1.0
2p	8.163	0.108 136
	1.6883	0.422 290
	0.3755	0.526 724
	0.1	0.240 748

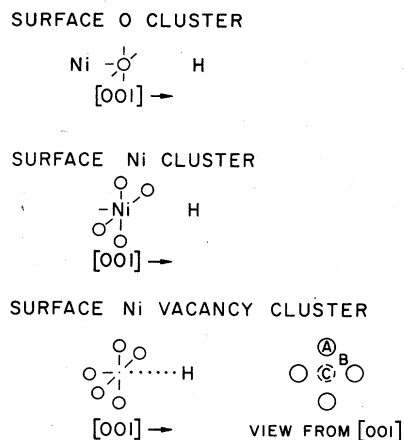


FIG. 1. Molecular clusters used to model various surface species. For the surface Ni vacancy *A* indicates the atop site, *B* the bridged, and *C* the centered.

quartet (RHF) curve lower. In addition, since *R*-O-H structures (*R* being some substituent) are usually bent, the bending of the NiOH was calculated for the minimum distance of the quartet curve, 3.85 a.u. These results are shown in Fig. 3. Note that the minimum is for 0° , which corresponds to perpendicular.

For the O_5 cluster representing the cation vacancy, we initially investigated the charge states for the cluster. Starting with the configuration O_5^{10-} , which corresponds to simply removing the Ni^{2+} ion, electrons were successively removed. These results are given in Table III. We find that the O_5^{9-} state is slightly below (0.13 eV) the O_5^{10-} state, the other states being higher. Furthermore, in the case of the O_5^{9-} , the electron is removed from a localized state, which is to say that the hole is localized on a given oxygen. The same is true of the two holes in the O_5^{8-} ($S_z = 1$) case.

Given the small energy spacing between the O_5^{10-} and O_5^{9-} surface states, we chose to investigate bonding to both configurations. The O_5^{10-} has no unpaired electrons on the surface and thus will

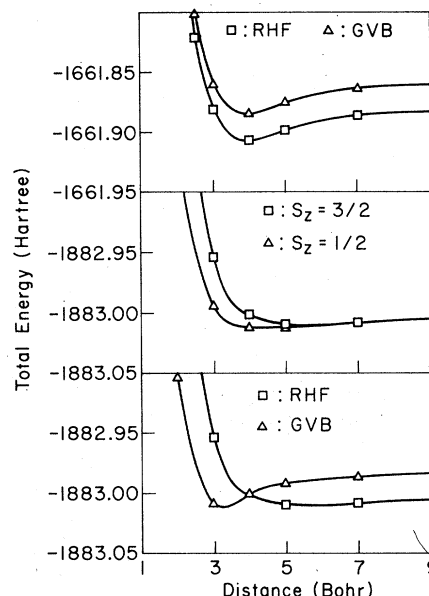


FIG. 2. Potential-energy curves for H atom approaching a surface O (NiOH) (top) and a surface Ni (O_4NiH) using UHF (middle) and RHF and GVB (bottom) wave functions.

give rise only to doublet states when coupled to a hydrogen. The O_5^{9-} has one unpaired electron, which can be coupled with the H electron to form a singlet or triplet. The doublet and triplet were calculated using an RHF wave function and are expected to be repulsive, while the singlet was calculated using a GVB wave function and should be attractive. As mentioned previously, three possible bonding sites were considered.

For the atop case, the results of the calculations are given in Fig. 4 and Table IV. As expected, the doublet and triplet curves produce essentially no bonding and look fairly similar to the Ni-O-H potential-energy curves. The singlet curve is a typical bonding potential-energy curve with a bond length of 1.72 a.u. and a binding energy of 5.30 eV. At large distance the surface GVB orbital is a

TABLE II. Calculated energies for the O_4 -Ni-H and Ni-O-H potential curves as a function of H distance from the surfaces. Energies and distances in Hartree a.u. The type of calculation and spin state are also indicated.

Distance (bohrs)	Energy NiOH			Energy O_4 -Ni-H		
	GVB (doublet)	RHF (quartet)	RHF (quartet)	GVB (doublet)	UHF ($S_z = \frac{3}{2}$)	UHF ($S_z = \frac{1}{2}$)
15.0	-1661.863 252	-1661.886 250	-1883.006 908	-1882.984 129	-1883.007 167	-1883.007 167
7.0	-1661.863 495	-1661.886 494	-1883.008 375	-1882.985 788	-1883.008 631	-1883.008 718
5.0	-1661.884 655	-1661.907 165	-1883.009 721	-1882.991 878	-1883.009 965	-1883.012 242
4.0	-1661.875 398	-1661.898 282	-1883.001 818	-1883.000 234	-1883.002 089	-1883.011 921
3.0	-1661.860 036	-1661.881 472	-1882.953 608	-1883.008 291	-1882.954 158	-1882.994 244
2.0	-1661.683 476	-1661.703 380	-1882.700 905	-1882.903 192	-1882.702 165	-1882.865 239

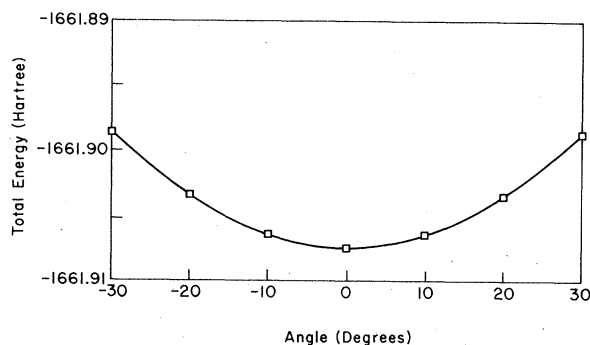


FIG. 3. Potential-energy curve for bending the Ni-O-H bond for an OH distance of 3.85 au. The angle is measured from the normal, hence 0° is linear.

$2p_x$ on the surface O; however, as the H approaches this orbital rotates into a $2p_z$ which bonds with the incoming H is orbital. In contrast, the singly occupied surface orbital in the triplet state remains a $2p_x$ at all distances.

For the bridged and center sites, the doublet and triplet curves are nonbonding as well (these are not shown). Their bonding curves, however, are markedly different from the atop case. These results are given in Fig. 5 and Table V. In the case of the bridged site, a partially ionic bond is formed between the two nearest oxygens and the hydrogen. The hydrogen loses about half of its electron density to the two surface oxygens. The GVB orbitals show a three center bond involving the two O's and the H, with each orbital localized more in one O-H bond, although polarized significantly toward the O. For the center site, the ionic character of the bond is even more marked. At 5 bohrs the H 1s orbital is still intact while at 3 bohrs it is significantly dissociated. By the time the H is in the plane, it is essentially a bare proton interacting with the O_5^{10-} structure (actually, just an ion in the Madelung well). The interesting portion of this curve occurs below the surface plane. As the H^+ moves back toward the second

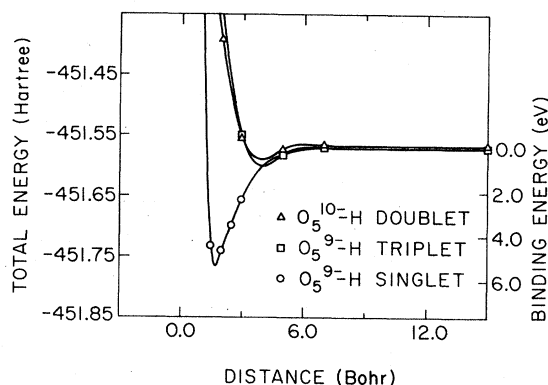


FIG. 4. Potential-energy curves for H approaching a surface Ni vacancy atop a surface O atom. The doublet curve corresponds to a complex of $5O^{2-}$, while the singlet and triplet curves correspond to $4O^{2-}1O^{-1}$.

layer O^{2-} , a covalent bond forms in which one electron from the O^{2-} moves onto the H. This gives rise to the flat part of the potential well and the small dip near -2.2 bohrs. Thus the distance of the minimum from the back oxygen is 1.70 bohrs.

At this point, the results for the corner site are quite predictable. The various charge states for the corner were calculated (Table VI), giving the state which is $2O^{2-}O^{1-}$ as the ground state. Again the centered or bridged sites will give rise to ionically bonded species as for the O_5 case. The most strongly bound curve is that for the atop site, which is given in Table VII. In Fig. 6 the O_3H and O_5H atop curves are compared. The O-H bond length at the equilibrium position for the O_3H is 1.73 a.u. and the binding energy is 7.34 eV. This curve, then, has a deeper minimum than the O_5 atop site but has a similar bond length.

IV. DISCUSSION

In Table VIII we give the binding energy and equilibrium bond distance for the various curves. There one sees that the "perfect-surface" calculations give much longer distances and weaker

TABLE III. Unrestricted Hartree-Fock energies for various electron occupancies for the surface Ni vacancy (O_5) cluster.

Cluster configuration	Unpaired electrons on surface	S_z	$\langle S^2 \rangle^a$	Total energy (Hartree)
$5O^{2-}$ (10-)	0	0	0.00	-451.068 846
$4O^{2-}1O^{1-}$ (9-)	1	$\frac{1}{2}$	0.50	-451.073 674
$3O^{2-}2O^{1-}$ (8-)	2	1	1.00	-450.931 014
$3O^{2-}2O^{1+}$ (8-)	2	0	0.62	-450.930 960

^a Evaluated from $\langle S^2 \rangle = S(S+1)$.

TABLE IV. RHF and GVB energies for the atop configuration of the O_5H cluster as a function of H distance from the surface.

Distance (bohrs)	Total energy (Hartree)		
	GVB (singlet)	RHF (triplet)	RHF (doublet)
15.0	-451.570 612	-451.570 610	-451.566 637
7.0	0.571 393	0.571 443	0.566 959
5.0	0.582 534	0.582 939	0.573 903
3.0	0.656 748	0.550 793	0.553 040
2.5	0.698 479
2.0	0.740 372	0.343 250	0.390 008
1.5	0.732 161
1.0	0.237 966

bonds than the defects. The GVB curve for O_4 -Ni-H gives a bond length of 3.27 a.u.; however, the corresponding UHF curve ($S_z = \frac{1}{2}$) gives a bond length of 4.99 a.u. This discrepancy can be understood by noting that the GVB curves for O_4 -Ni-H and Ni-O-H are both 0.62 eV above the corresponding RHF curve for large R . Also note that the UHF curves approach the same asymptotic energy. The problem is that the GVB wave function is constrained to use one of two possible doublet spin-eigenfunctions, while the UHF wave function is not. Using a more general form of the GVB wave function would alleviate this problem. Finally, if we compare the Ni-H and O-H distances for the perfect surface with molecular NiH and OH, whose molecular bond lengths are 2.79 and 1.83 a.u., respectively,¹² we find that these are much shorter than those obtained for the perfect surface.

For the atop sites for both the O_5H and O_3H clusters, the bond length is ~ 1.72 a.u. As can be seen in Fig. 6, however, the curves for these two cases are somewhat different. The corner produces a much stronger bond, 7.34 eV, than the surface, 5.30 eV. The vibrational frequencies for the two curves, in the harmonic approximation, are 4302 cm^{-1} for the corner and 5303 cm^{-1} for the surface. The bond length and vibrational frequency for OH^- are 1.83 a.u. and 3740 cm^{-1} .¹³ Thus we find that the bond lengths to the defects are shorter and the

TABLE VI. Restricted Hartree-Fock energies for various electron occupancies for the Ni corner vacancy (O_3) cluster.

Cluster configuration	Unpaired electrons on defect	S_z	Total energy (Hartree)
$3O^{2-}$ (6-)	0	0	-303.788 859
$2O^{2-}O^{1-}$ (5-)	1	$\frac{1}{2}$	-303.830 015
$O^{2-}O^{1-}$ (4-)	2	1	-303.635 412
$3O^{1-}$ (3-)	3	$\frac{3}{2}$	-303.333 251

TABLE V. GVB energies for the bridged and center configurations of the O_5H cluster as a function of H distance from the surface.

Distance (bohrs)	Total energy (Hartree)	
	Bridged	Center
15.0	-451.570 627	-451.570 155
7.0	0.570 671	0.570 727
5.0	0.577 329	...
3.0	0.613 771	0.625 824
2.0	0.677 171	0.725 441
1.0	0.724 178	0.802 688
0.0	0.733 897	0.835 637
-1.0	0.705 478	0.839 311
-2.0	...	0.848 309
-2.5	...	0.789 598

bonds are "stiffer." This may be due, in part, to the partially ionic nature of the bonding in both instances. The incomplete long-range potential overestimates the Madelung potential leading to a slight overbinding. Finally, a more flexible basis set may change the calculations somewhat. The point remains that regardless of these provisos, the nature and magnitude of bonding will not change substantially. For the atop sites on the defects, then, one finds a structure that is essentially an OH^- molecular ion. For the bridged and center surface sites, we have already pointed out that the bonding is essentially ionic.

While this study is not designed to give the mechanism for H_2 dissociation on NiO, certain observations with regard to the energetics can be made. Given that the dissociation energy for H_2 is 4.476 eV,¹² forming one bond of greater energy or two bonds of more than half the dissociation energy is energetically favorable. For the perfect surface this will never be the case. For the defects, there is always enough energy in a single bond to dissociate an H_2 .

The dissociative chemisorption of H_2 on oxygen sites on NiO is consistent with the experimental

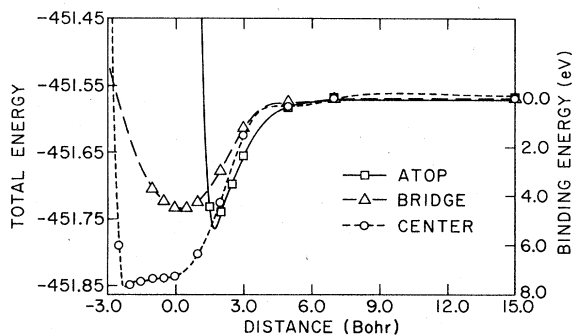


FIG. 5. Singlet (GVB) potential-energy curve for H approaching a surface Ni vacancy in three different configurations.

TABLE VII. GVB energies for the atop configuration of the O_3H cluster as a function of H distance.

Distance (bohrs)	Total energy (Hartree)
15.0	-304.327 648
7.0	-304.328 413
5.0	-304.343 771
3.0	-304.470 882
2.5	-304.527 453
2.0	-304.579 919
1.5	-304.573 735
1.0	-303.781 419

data of Charman and Dell.² They studied the chemisorption of H_2 and O_2 on unirradiated and neutron irradiated NiO and MgO. For the unirradiated materials they found some activity in NiO but little in MgO. Upon irradiation there is an increased activity on both substances, that on MgO being more striking. At room temperature the adsorption is separated into a fast reversible part, a fast irreversible part, and a slow part. The irradiation causes the greatest increase in the fast irreversible adsorption, the slow adsorption being somewhat enhanced and the fast reversible adsorption only changing with very high neutron doses. Furthermore, a given material behaves similarly for H_2 and O_2 . They suggest that this is due to the formation of equal numbers of oxygenlike and metal-like defects, with the hydrogen chemisorption

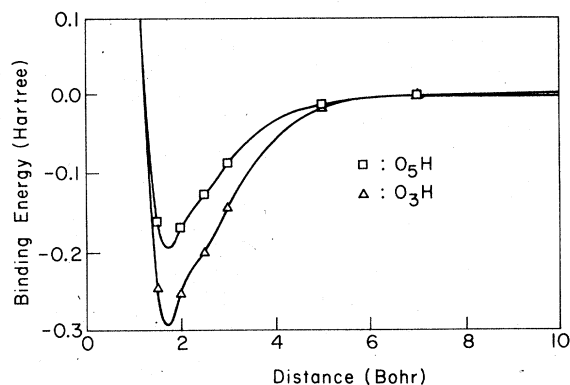


FIG. 6. Binding-energy curve for H approaching atop an O for the corner and surface Ni vacancies in NiO.

occurring on the oxygen-rich sites and the oxygen chemisorption occurring on the metallic sites. We would interpret the fast irreversible adsorption as being due to cation vacancy sites in both materials. The activity of unirradiated NiO is probably due to the samples being less stoichiometric in the case of NiO. The slow adsorption increase could well be due to diffusion into interior defects. Whether or not the oxygen activity is due to complementary cation sites remains a point of conjecture.

V. CONCLUSION

We find that for H to bind to a NiO surface, it is necessary to introduce some change in the surface

TABLE VIII. Binding energies and equilibrium bond distances for H approaching various surface and defect sites on NiO.

Cluster	Wave function used	Electronic ^a state	Binding energy ^b (eV)	Equilibrium distance (a.u.)
NiOH	RHF	Quartet	0.606	3.82
	GVB	Doublet	0.579	3.85
O_4NiH	RHF	Quartet	0.106	5.66
	GVB	Doublet	0.753	3.27
	UHF	Quartet	0.113	5.66
	UHF	Doublet	0.138	4.99
O_5H (atop)	GVB	Singlet	5.30	1.72
	GVB	Singlet	4.47	0.24 ^b
	GVB	Singlet	7.72	-2.23 ^b
O_3H (atop)	GVB	Singlet	7.34	1.73

^a For UHF calculations this is S_z .

^b As measured from the surface plane. In these cases there is no atom along the specific [001] direction of the H atom in the surface plane.

electronic structure. That is, for the case of Ni^{2+} and O^{2-} ions on the "perfect" surface, there is no binding. However if a defect is introduced, the defect changes the local electronic structure, giving rise to chemical activity. We find this to be true for the (001) surface of NiO and for a cube edge. For the specific cases studied here, we find that cation vacancies lead to the formation of OH^- structures on the surface which are quite strongly bound (5–7 eV), but are otherwise similar to OH^- radicals. While we have not specifically

investigated the mechanism for H_2 dissociation, we have established that this reaction would be energetically favorable on the defects but not on the "perfect" surface.

ACKNOWLEDGMENT

This work is supported in part by the NSF under MRL Grant No. DMR-76-01058 and by the U. S. AFOSR under Grant No. AFOSR-76-2989.

¹P. C. Gravelle and S. J. Teichner, *Adv. Catal.* **20**, 167 (1969).

²H. B. Charman, R. M. Dell, and S. S. Teale, *Trans. Faraday Soc.* **59**, 453 (1963); H. B. Charman and R. M. Dell, *ibid.* **59**, 470 (1963).

³G. T. Surratt and A. B. Kunz, *Phys. Rev. Lett.* **40**, 347 (1978).

⁴G. T. Surratt and A. B. Kunz, *Solid State Commun.* **23**, 555 (1977).

⁵D. L. Klein, G. T. Surratt, and A. B. Kunz (unpublished).

⁶M. P. Guse, R. J. Blint, and A. B. Kunz, *Int. J. Quantum Chem.* **9**, 725 (1977); C. F. Melius, A. P. Mortolla, M. B. Baille, and M. A. Ratner, *Surf. Sci.* **59**, 279 (1976).

⁷J. E. Demuth, *Surf. Sci.* **65**, 369 (1977).

⁸J. C. Slater, *Quantum Theory of Molecules and Solids* (McGraw-Hill, New York, 1965), Vol. II.

⁹W. J. Hunt, P. J. Hay, and W. A. Goddard, III, *J. Chem. Phys.* **97**, 738 (1972).

¹⁰H. Basch, C. J. Hornback, and J. W. Moskowitz, *J. Chem. Phys.* **51**, 1311 (1969).

¹¹A. B. Kunz and M. P. Guse, *Chem. Phys. Lett.* **45**, 18 (1977).

¹²G. Herzberg, *Molecular Spectra and Molecular Structure* (Van Nostrand, New York, 1950), Vol. 1.

¹³G. Herzberg, *The Spectra and Structure of Simple Free Radicals* (Cornell University, Ithaca, 1971).